

Published in final edited form as:

*Anat Rec (Hoboken)*. 2010 May ; 293(5): 821–828. doi:10.1002/ar.21103.

## Molecular Morphology of the Chick Heart Visualized by MALDI Imaging Mass Spectrometry

Angus C. Grey<sup>1,\*</sup>, Andrew K. Gelasco<sup>1</sup>, Jarren Section<sup>1</sup>, Ricardo A. Moreno-Rodriguez<sup>2</sup>, Edward L. Krug<sup>2</sup>, and Kevin L. Schey<sup>1,\*</sup>

<sup>1</sup> Department of Cell and Molecular Pharmacology, Medical University of South Carolina, Charleston, South Carolina

<sup>2</sup> Department of Cell Biology and Anatomy, Medical University of South Carolina, Charleston, South Carolina

### Abstract

Utilization of MALDI-MS (matrix-assisted laser desorption/ionization mass spectrometry) for tissue imaging is a relatively new proteomic technique that simultaneously maps the spatial distribution of multiple proteins directly within a single frozen tissue section. Here we report the development of a methodology to apply MALDI tissue imaging to chick heart tissue sections acquired from fixed and paraffin-embedded samples. This protocol produces molecular images that can be related to the high quality histological tissue sections.

Perfused term chick hearts were fixed in acidic ethanol and embedded in paraffin wax. Tissue sections (15  $\mu\text{m}$ ) were collected onto conductive slides, deparaffinized with xylene and transitioned into water with graded ethanol washes and allowed to air dry. In separate experiments three different MALDI matrices were applied to chick heart tissue sections through repeated cycles from a glass nebulizer. Tissue sections were then analyzed by MALDI mass spectrometry using a raster step-size of 75–100  $\mu\text{m}$ , and molecular images for specific  $m/z$  ratios reconstituted.

MALDI tissue imaging revealed spatially-resolved protein signals within single heart sections that are specific to structures or regions of the heart, e.g., vessels, valves, endocardium, myocardium, or septa. Moreover, no prior knowledge of protein expression is required as is the case for immunohistochemistry and *in situ* hybridization methodologies. The ability to simultaneously localize a large number of unique protein signals within a single tissue section, with good preservation of histological features, provides cardiovascular researchers a new tool to give insight into the molecular mechanisms underlying normal and pathological conditions.

### Keywords

MALDI tissue imaging; proteomics; heart; morphology

## INTRODUCTION

Detection of protein expression patterns by immunohistochemistry is a standard research tool for investigating the localization of specific antigens in tissues. The technical basis of such studies requires prior knowledge of the particular proteins of interest and relies on either commercial or investigator-derived antibodies. Ideally each antibody should recognize

\*Current Address and Address for correspondence: Kevin L. Schey, Mass Spectrometry Research Center, Vanderbilt University, 465 21<sup>st</sup> Ave. So., Suite 9160 MRB III, Nashville, TN 37232-8575, USA. Phone: 615-936-6861, Fax: 615-343-8372, kevin.schey@vanderbilt.edu.

only its intended antigen, but in practice many have some degree of cross-reactivity with other proteins. While this is relatively straightforward to demonstrate for immunoblotting methods, it is much more difficult to show absolute selectivity for immunohistochemistry. Physical accessibility of the epitope can also be an issue, requiring “epitope retrieval” strategies to unmask antigenic sites.(D’Amico et al., 2009) Expanding histological analysis to the simultaneous localization of multiple proteins in the same section brings additional complications of limited primary/secondary antibody pairings due to source species and the availability of spectrally-distinct fluorophores. In general, the relative distribution of only two to three proteins can be evaluated in any one tissue section. Given that the “omics” era of science produces a multitude of targets that could be involved in the molecular events preceding the overt morphological phenotypes of diseases and pathologies, it is unrealistic to conceive of generating specific immunoreagents to all of these proteins and any related post-translational modifications that might occur, let alone using conventional immunohistochemical methods to evaluate their relative distributions.

Mass spectrometry is currently the most sensitive technology for discriminating protein identities by mass differences of only a few daltons. MALDI-MS (matrix-assisted laser desorption/ionization mass spectrometry) imaging mass spectrometry, or “MALDI tissue imaging,” is a relatively new proteomic technique that simultaneously maps the spatial distribution of multiple proteins directly in a single tissue section. The experimental workflow for a MALDI imaging experiment is shown schematically in Figure 1. Typically, frozen tissue is sectioned to 10–20  $\mu\text{m}$  thickness, transferred to either a conductive MALDI sample plate or conductive glass slide, coated with matrix solution, and analyzed by MALDI mass spectrometry. During data collection, the MALDI laser is raster scanned across the tissue section with user-defined spatial resolution, typically 100–200  $\mu\text{m}$  in  $x$  and  $y$  dimensions, and a mass spectrum collected at each sampling location. Depending on whether matrix solution is applied by glass nebulizer/airbrush(Garrett et al., 2007) or automatically,(Aerni et al., 2006; Baluya et al., 2007; Deininger et al., 2008) 10’s to 1000’s of peptide and protein signals are observed simultaneously in a single experiment.. Generally, soluble peptides and proteins in the mass-to-charge ( $m/z$ ) range 3,000 – 30,000 are detected, although efforts to extend the detectable mass range to higher  $m/z$  are ongoing. (Leinweber et al., 2009) To interpret the data, the intensity of any  $m/z$  signal observed in the mass spectral data is plotted as a function of sampling position, where each  $m/z$  signal represents a protein, protein form or peptide, and each sampling position represents one pixel in the resultant display. In this way, two-dimensional ion density maps, or molecular images, can be reconstituted for any observed  $m/z$  signal. This technique has distinct advantages over traditional MALDI mass spectrometry analysis, such as no protein extraction and separation procedures, minimal sample preparation, and the maintenance of spatial information. Signal/protein identification can then be determined using standard proteomics approaches.

First used to detect proteins and peptides in rat pancreas and pituitary (Caprioli et al., 1997), MALDI tissue imaging has now been applied to isolated tissues as varied as the mouse brain(Stoeckli et al., 2001), bovine lens(Han and Schey, 2006), and cancerous human lung(Yanagisawa et al., 2003), and from single neuronal cells(Rubakhin et al., 2003) to whole body analysis (Khatib-Shahidi et al., 2006; Stoeckli et al., 2007; Trim et al., 2009). Direct tissue analysis by MALDI can detect a variety of analytes; phospholipids,(Rujoi et al., 2004; Sjövall et al., 2004; Jackson et al., 2005; Woods and Jackson, 2006; Jackson et al., 2007)pharmaceuticals,(Troendle et al., 1999; Reyzer et al., 2003; Signor et al., 2007; Chen et al., 2008; Liu et al., 2009; Trim et al., 2009) peptides,(DeKeyser et al., 2007; Groseclose et al., 2007; Rubakhin et al., 2007; Taban et al., 2007; Minerva et al., 2008; Monroe et al., 2008) and proteins(Stoeckli et al., 2001; Yanagisawa et al., 2003; Han and Schey, 2006) have all been successfully detected in a spatially distinct manner. Normally, fresh-frozen

tissue is analyzed, although recent advances have made biochemical information accessible from formalin-fixed paraffin-embedded (FFPE) samples via *in situ* enzymatic digestion (Lemaire et al., 2007), with subsequent application to disease marker identification. (Groseclose et al., 2008; Stauber et al., 2008) Here we report the application of MALDI tissue imaging to study protein localization in heart tissue that includes the development of a tissue preparation protocol that utilizes ethanol/acetic acid fixation and paraffin-embedded sectioning yielding improved retention of histological features over traditional frozen section preparations used for MALDI tissue imaging. Furthermore, the use of ethanol/acetic acid fixation eliminates crosslinking artifacts and signal suppression generated by formalin fixation protocols. Using this technique, we observed a multitude of peptide and protein signals in deparaffinized chick heart tissue sections prepared for MALDI tissue imaging with any of three MALDI matrices examined. Protein signals can be detected that are specific for the major heart vessels, valves, endocardium, or septa, and can be distinguished from those expressed throughout the myocardium without any prior knowledge of which proteins might be present. Thus, the combination of MALDI tissue imaging with acid-alcohol fixed tissue is a powerful new analytical tool for resolving the relative spatial expression dynamics of a large number of different proteins and modifications simultaneously in a single section of heart tissue. This gives cardiovascular researchers the potential of an integrated readout of the molecular mechanisms underlying normal and pathological conditions.

## MATERIALS AND METHODS

### Reagents

Acetonitrile, high-performance liquid chromatography (HPLC)-grade water, and trifluoroacetic acid were purchased from Thermo Fisher Scientific Inc. (Hampton, NH). Phosphate-buffered saline (PBS) tablets, 3,5-dimethoxy 4-hydroxycinnamic acid (sinapinic acid, SA), and  $\alpha$ -cyano-4-hydroxycinnamic acid (CHCA) were purchased from Sigma-Aldrich (St Louis, MO). Indium tin oxide-coated conductive glass microscope slides and 2,5-dihydroxybenzoic acid (DHB) MALDI matrix were purchased from Bruker Daltonics (Billerica, MA). Unless otherwise stated all other chemicals were obtained from Sigma-Aldrich.

### Tissue preparation

Hatching chicks (*Gallus gallus domesticus*, Pilgrim's Pride, Sumter, SC) were sacrificed by cervical dislocation and their hearts removed and washed in PBS several times. The heart was then perfused thoroughly with ice cold PBS (10–15 mL over 2–3 min) in order to remove residual internal blood. Additionally, PBS was injected into the coronary sinus to rid blood from the coronary veins. Whole chick hearts were immersed in a  $-20^{\circ}\text{C}$  solution of 75% ethanol and 25% glacial acetic acid for 24 hours. On the next day, they were changed to 80% ethanol for 2 hours, then 90% ethanol for 5 hours, and then to 100% ethanol for 1–2 days. Following the dehydrating process, the hearts were transferred to xylene for two washes, until the heart appeared to be transparent. The samples were pre-included in paraffin overnight in a vacuum oven at  $55\text{--}56^{\circ}\text{C}$ . They were then transferred to paraffin for one hour at  $55\text{--}56^{\circ}\text{C}$  then oriented to make frontal sections and the paraffin allowed to harden. All paraffin-embedded tissues were sectioned at  $15\mu\text{m}$  thickness. After sectioning, each individual section was transferred to a conductive glass slide by dotting the slide with water, and then warming the slide on a hot plate to  $60^{\circ}\text{C}$ , allowing the floating sections to settle and flatten on the slides. The water was removed and the slide was allowed to dry for one to two days. The dry sections were heated to  $70^{\circ}\text{C}$  for 2 seconds in order to melt the paraffin, which was then removed by soaking in xylene for 24 hours. The deparaffinized sections were processed through 100% ethanol (3 washes, 10 minutes each), then transferred to 70%

ethanol (10 minutes), washed with water (3 times, 10 minutes each), and then allowed to air dry for 2 hours.

### MALDI matrix deposition

MALDI matrices were dissolved in 70% acetonitrile/0.1% trifluoroacetic acid. DHB was used at a concentration of 40 mg/ml, while CHCA and SA were used at a concentration of 15 mg/ml. Matrix solution was applied to dry chick heart tissue sections through repeated cycles from a glass nebulizer until an even coating of matrix crystals across the entire tissue slice was achieved. After drying, tissue sections were analyzed by MALDI mass spectrometry.

### Mass Spectrometry

Mass spectrometric analyses were performed in the linear, positive mode at +20 kV accelerating potential on a time-of-flight mass spectrometer (Bruker Autoflex III TOF-TOF; Bruker Daltonik, Bremen, Germany), which was equipped with a Smartbeam laser capable of operating at a repetition rate of 200 Hz with optimized delayed extraction time and laser beam size was set to medium. Laser energy was optimized for signal-to-noise in each preparation. Using Bruker Protein Standard 1 (Bruker Daltonik, Bremen, Germany), a linear external calibration was applied to the instrument prior to data collection. Mass spectral data sets were acquired over a whole chick heart section using flexImaging™ software (Bruker Daltonik, Bremen, Germany) in the mass range of  $m/z$  3,000 to 30,000, with a raster step size of 75 or 100  $\mu\text{m}$  and 250 laser shots per spectrum. After data acquisition, molecular images were reconstituted using the flexImaging™ software. Each data set consists of approximately 6,000 individual sampling locations, or pixels. Data was normalized using flexImaging™ software, and each  $m/z$  signal plotted  $\pm 4$  mass units for  $m/z$  values < 7000,  $\pm 6$  mass units for  $m/z$  values 7000–10000, and  $\pm 8$  mass units for  $m/z$  values > 10000. For display purposes, data was interpolated and pixel intensities were rescaled in flexImaging™ to utilize the entire dynamic range.

## RESULTS

Tissue preparation for MALDI tissue imaging involves several straightforward yet critical steps in order to acquire high quality data. Traditionally, frozen sections have been utilized in MALDI tissue imaging, and although each tissue requires optimization of experimental conditions for best results, standardized MALDI tissue imaging workflows have been reported.(Chaurand et al., 2006; Kaleta et al., 2009) In addition, techniques have been developed to acquire tissue images from paraformaldehyde-fixed, paraffin-embedded tissue, with good success.(Lemaire et al., 2007) More recently, protocols for the acquisition of tissue images from ethanol-fixed, paraffin embedded lung tissue sections (Chaurand et al., 2008) and matrix solution fixation of cryosectioned brain tissue (Agar et al., 2007) have been reported. We have developed a similar technique, instead utilizing acidified ethanol fixation, which combines high-quality anatomical information gained from non-chemically fixed, paraffin-embedded tissue sectioning, with deparaffinization and matrix solvent conditions optimized for high-quality molecular images of chick heart tissue. Many attempts to employ standard frozen section protocols to chick heart MALDI tissue imaging (Chaurand et al., 2006) yielded poor maintenance of anatomical features (Supplemental Figure S1) and most often lower mass spectral quality (Supplemental Figure S2).

In the present study multiple peptide and protein signals were observed when any of the common MALDI matrices DHB, CHCA, or SA were spray deposited. The different matrices were used to gain complementary mass spectral information, a strategy which has been employed in other studies.(Khatib-Shahidi et al., 2006; Andersson et al., 2008) For

example, CHCA typically provides improved signal at low mass while SA provides better signal at higher molecular masses. Protein signals common and unique to each matrix system were observed (compare spectra in Figure 2 to Supplemental Figure S2). The most abundant protein signals detected in each preparation generally showed a ubiquitous localization. However, many protein signals with spatially distinct localization were also detected, and are the focus of the following discussion.

Figure 2 shows two average MALDI mass spectra, acquired with CHCA matrix, extracted from an image data set from two distinct regions of interest. Many signals are observed; any of which can be plotted as a function of location to produce a plethora of images from a single imaging experiment. The main differences in protein expression are highlighted by changes in mass spectral signals highlighted in the spectra.

Molecular images for four spatially distinct  $m/z$  signals in a single section of chick heart tissue prepared with DHB matrix, each representing a unique protein, are presented in Figure 3, along with the corresponding optical image (Figure 3F). A signal at  $m/z$  6614 was found predominantly in the myocardium of the right ventricle (Figure 3A), whereas signals at  $m/z$  7475 and  $m/z$  6143 were localized predominantly to the walls of the major heart vessels (Figure 3B and 3C, respectively). Interestingly,  $m/z$  7475 and  $m/z$  6143 were localized to different layers in the major heart vessels, as shown in the merged image of  $m/z$  6614,  $m/z$  7475, and  $m/z$  6143, where each  $m/z$  signal is displayed as a distinct monochromatic pseudocolor (Figure 3D). This pattern indicates the known molecular heterogeneity and layered arrangement of the major heart vessels, and demonstrates the ability of MALDI tissue imaging to accurately detect regional differences in protein distribution throughout cardiac tissue. In contrast, a signal at  $m/z$  6669 was found at low levels in all regions of the tissue slice and highly expressed at other sites including the apex of the interventricular septum (Figure 3E).

Spatially distinct patterns for several  $m/z$  signals were also observed when CHCA was used as matrix (Figure 4). A protein signal at  $m/z$  9329 was localized to the bundle of His and it appears to descend the interventricular septum (Figure 4A). In contrast, a signal at  $m/z$  9492 was distributed at intermediate levels throughout the myocardium of both the atria and ventricles, but was more intense in the interventricular septum (Figure 4B). A signal at  $m/z$  11862 was also found at intermediate levels in the atrial and right ventricular myocardium, and localized strongly to major heart vessels and sporadically as intense foci within the free walls of both ventricles (possibly coronary vasculature) (Figure 4C). Interestingly, a signal at  $m/z$  12209 was localized exclusively to heart valve structures (Figure 4D). The spatial relationship of each  $m/z$  signal is evident in the merged image (Figure 4E). In particular, this display mode shows  $m/z$  11862 localized to coronary arteries embedded in the interventricular septum (Figure 4E, arrowheads), which are clearly visible in the optical scan of the tissue section (Figure 4F) and the distinct signal in the bundle of His (white).

Both the spatial resolution of the method and the reproducibility of the sample preparation method are demonstrated by the images presented in Figure 5. Using four serial sections coated with SA matrix the same distribution of signals can be seen for the four  $m/z$  values displayed. The signal at  $m/z$  3915 (blue) is confined to the leaflets of the left ventricular A–V valve and shows high spatial resolution. The signal at  $m/z$  5308 (green) localizes to aortic valvular tissue which is spatially distinct from the signal at  $m/z$  5935 (red) corresponding to aortic intimal or adventitial tissue. The spatially restricted expression of both signals is apparent in all four serial sections. The signal at  $m/z$  6643 (pink) is localized throughout the atrial myocardium and outer ventricular wall.



## DISCUSSION

MALDI tissue imaging is a new analytical technique that has already been used to investigate the tissue distribution of molecules as varied as pharmaceuticals, lipids and proteins in many tissue types. In this study, a tissue preparation procedure that utilizes deparaffinized tissue sections with high quality anatomical information that can be prepared for MALDI tissue imaging has been developed. This protocol was based on standard techniques utilized for immunohistochemical staining of chick heart tissue, which aims to maintain anatomical structures and antigenic sites for subsequent antibody labelling. The potential of ethanol fixed/paraffin embedded tissue for proteomic analysis has previously been demonstrated.(Gillespie et al., 2002) Furthermore, similar, albeit shorter, paraffin removal steps have been utilized to prepare FFPE tissue microarrays for MALDI tissue imaging and subsequent biomarker identification in squamous cell carcinoma.(Groseclose et al., 2008) Therefore the current protocol is not predicted to significantly degrade the quality of the observed proteomic information. Using this protocol, multiple protein signals with spatially distinct distribution patterns were observed in a single tissue section of the chick heart. This is to be expected, since the differential molecular make up of cardiac structures as diverse as myocardium, vascular smooth muscle, adventitia and other connective tissue is well known. The power of the MALDI imaging method is that these signals can be acquired simultaneously and in a “discovery-mode” where prior knowledge of proteins to be imaged is not required. Moreover, post-translationally modified proteins can be imaged;(Han and Schey, 2006; Grey and Schey, 2008) a challenging prospect for alternative imaging methods.

The MALDI imaging approach has a bias toward soluble lower molecular weight (< 50kDa) proteins, however, this limitation can be overcome to some extent by alternative means of sample preparation(Leinweber et al., 2009) and by trypsin treatment.(Groseclose et al., 2007) The spatial resolution achieved in MALDI imaging is generally limited by the laser diameter and the matrix deposition. However, modified sampling techniques have been reported that increase MALDI imaging spatial resolution,(Jurchen et al., 2005; Zimmerman et al., 2008) and continued instrumentation development will increase MALDI imaging spatial resolution. Although sub-cellular protein expression cannot be routinely resolved as with optical microscopy, important anatomical features are clearly identifiable as demonstrated in the current figures.

In the present study, using common MALDI matrices, the relative spatial relationships of multiple protein signals were observed in heart tissue sections with good reproducibility. Both the matrix and solvent system used for MALDI tissue imaging dictate which protein signals are detected in each mass spectrum. The observation of different protein signals in each preparation is most likely due to a combination of the different matrices used and the different anatomical locations from which the sections were obtained. Interestingly, the molecular mass sampling bias of MALDI imaging mass spectrometry to soluble proteins in the range below  $m/z$  30,000 favours localization of proteins that may not be detectable by commercially available antibodies. A survey of immunological reagents that detect cardiac antigens from AbCam Inc. revealed a range in antigen mass from a few thousand to over three million daltons, the majority of which were related to the cytoskeleton, extracellular matrix, or gap junctions. Only 23 of the 124 antigens were less than 30,000 daltons, suggesting that this lower mass bias of MALDI imaging yields protein signatures that do not correlate with most proteins traditionally studied by immunohistochemical methods. Identification of the corresponding proteins may yield new insight into regulation of tissue differentiation and function.

MALDI tissue imaging is also being used as a protein discovery tool, with particular application to biomarker discovery, for example in cancerous tissues. (Yanagisawa et al., 2003; Groseclose et al., 2008; Stauber et al., 2008) In heart tissue, changes in protein expression during development or during pathogenesis can be detected with this technology, however, once observed and reproduced, the biomarker signal must be identified. There are several methods to do this. First, a traditional proteomic approach may be used to acquire sequence information, e.g., tissue homogenization, protein extraction, enzymatic digestion, peptide chromatography followed by tandem mass spectrometry analysis. Protein databases can then be interrogated with observed data and proteins identified. While this approach is fairly standard in proteomics laboratories, it can be laborious. Extraction of the protein signals of interest can be challenging, and spatial resolution is difficult to maintain. Combining laser capture microdissection with standard proteomics methods should prove a useful tool to identify imaged signals. More recently, *in situ* protein digestion has been demonstrated as a method to identify proteins observed in MALDI tissue imaging. (Groseclose et al., 2007; Lemaire et al., 2007) In this experiment, microdroplets of a proteolytic enzyme are deposited on to the surface of tissue slices in a dense array in *x* and *y*, followed by matrix solution. MALDI tissue imaging data is collected, and molecular images of detected peptides are reconstituted. In addition, detected peptides can be subjected to tandem mass spectrometry directly from tissue sections to acquire sequence information, which can be used in a subsequent database search to identify detected peptides/proteins.

The current study reports the establishment of a MALDI tissue imaging methodology for chick heart tissue and creates a baseline measurement of the normal chick heart proteome. Future studies will involve applying this methodology to molecularly characterize stages of heart development and to compare MALDI images of hearts from gene-targeted mice with known cardiovascular defects to assess the earliest variation in the spatial relationships of protein signals similar to those identified in this report. This information can now be used to follow the course of normal and anomalous cardiac development in order to gain a greater understanding of structure/function relationships of cardiac proteins.

## Supplementary Material

Refer to Web version on PubMed Central for supplementary material.

## Acknowledgments

**Sources of Funding:** This work was conducted in a facility constructed with support from the National Institutes of Health, Grant Number C06 RR018823 from the Extramural Research Facilities Program of the National Center for Research Resources, and supported by the NIH NHLBI Cardiovascular Proteomics Center Contract N01-HV-28282. A Summer Undergraduate Research Program Grant, NIH grant T35HL007769, is also acknowledged.

## References

- Aerni HR, Cornett DS, Caprioli RM. Automated acoustic matrix deposition for MALDI sample preparation. *Analytical Chemistry*. 2006; 78:827–834. [PubMed: 16448057]
- Agar NYR, Yang HW, Carroll RS, Black PM, Agar JN. Matrix solution fixation: Histology-compatible tissue preparation for MALDI mass spectrometry. *Analytical Chemistry*. 2007; 79:7416–7423. [PubMed: 17822313]
- Andersson M, Groseclose MR, Deutch AY, Caprioli RM. Imaging mass spectrometry of proteins and peptides: 3D volume reconstruction. *Nature Methods*. 2008; 5:101–108. [PubMed: 18165806]
- Baluya DL, Garrett TJ, Yost RA. Automated MALDI matrix deposition method with inkjet printing for imaging mass spectrometry. *Analytical Chemistry*. 2007; 79:6862–6867. [PubMed: 17658766]

- Caprioli RM, Farmer TB, Gile J. Molecular imaging of biological samples: localization of peptides and proteins using MALDI-TOF MS. *Analytical Chemistry*. 1997; 69:4751–4760. [PubMed: 9406525]
- Chaurand P, Latham JC, Lane KB, Mobley JA, Polosukhin VV, Wirth PS, Nanney LB, Caprioli RM. Imaging mass spectrometry of intact proteins from alcohol preserved tissue specimens: bypassing formalin fixation. *Journal of Proteome Research*. 2008 in press.
- Chaurand P, Norris JL, Cornett DS, Mobley JA, Caprioli RM. New developments in profiling and imaging of proteins from tissue sections by MALDI mass spectrometry. *Journal of Proteome Research*. 2006; 5:2889–2900. [PubMed: 17081040]
- Chen J, Hsieh Y, Knemeyer I, Crossman L, Korfmacher WA. Visualization of first-pass drug metabolism of terfenadine by MALDI-imaging mass spectrometry. *Drug Metabolism Letters*. 2008; 2:1–4. [PubMed: 19356062]
- D'Amico F, Skarmoutsou E, Stivala F. State of the art in antigen retrieval for immunohistochemistry. *Journal of Immunological Methods*. 2009; 341:1–18. [PubMed: 19063895]
- Deininger S-O, Ebert MP, Futterer A, Gerhard M, Rocken C. MALDI imaging combined with hierarchical clustering as a new tool for the interpretation of complex human cancers. *Journal of Proteome Research*. 2008; 7:5230–5236. [PubMed: 19367705]
- DeKeyser SS, Kutz-Naber KK, Schmidt JJ, Barrett-Wilt GA, Li L. Imaging mass spectrometry of neuropeptides in decapod crustacean neuronal tissues. *Journal of Proteome Research*. 2007; 6:1782–1791. [PubMed: 17381149]
- Garrett TJ, Prieto-Conaway MC, Kovtoun V, Bui H, Izgarian N, Stafford G, Yost RA. Imaging of small molecules in tissue sections with a new intermediate-pressure MALDI linear ion trap mass spectrometer. *International Journal of Mass Spectrometry*. 2007; 260:166–176.
- Gillespie JW, Best CJM, Bichsel VE, Cole KA, Greenhut SF, Hewitt SM, Ahram M, Gathright YB, Merino MJ, Strausberg RL, Epstein JI, Hamilton SR, Gannot G, Baibakova GV, Calvert VS, Flaig MJ, Chuaqui RF, Herring JC, Pfeifer J, Petricoin EF, Linehan WM, Duray PH, Bova GS, Emmert-Buck MR. Evaluation of non-formalin tissue fixation for molecular profiling studies. *American Journal of Pathology*. 2002; 160:449–457. [PubMed: 11839565]
- Grey AC, Schey KL. Distribution of bovine and rabbit lens alpha-crystallin products by MALDI imaging mass spectrometry. *Molecular Vision*. 2008; 14:171–179. [PubMed: 18334935]
- Groseclose MR, Andersson M, Hardesty WM, Caprioli RM. Identification of proteins directly from tissue: in situ tryptic digestions coupled with imaging mass spectrometry. *Journal of Mass Spectrometry*. 2007; 42:254–262. [PubMed: 17230433]
- Groseclose MR, Massion PP, Chaurand P, Caprioli RM. High-throughput proteomic analysis of formalin-fixed paraffin-embedded tissue microarrays using MALDI imaging mass spectrometry. *Proteomics*. 2008; 8:3715–3724. [PubMed: 18712763]
- Han J, Schey KL. MALDI tissue imaging of ocular lens  $\alpha$ -crystallin. *Investigative Ophthalmology and Visual Science*. 2006; 47:2990–2996. [PubMed: 16799044]
- Jackson SN, Wang H-YJ, Woods AS. In situ structural characterization of glycerophospholipids and sulfatides in brain tissue using MALDI-MS/MS. *Journal of the American Society for Mass Spectrometry*. 2007; 18:17–26. [PubMed: 17005416]
- Jackson SN, Wang HYJ, Woods AS. Direct profiling of lipid distribution in brain tissue using MALDI-TOF MS. *Analytical Chemistry*. 2005; 77:4523–4527. [PubMed: 16013869]
- Jurchen JC, Rubakhin SS, Sweedler JV. MALDI-MS imaging of features smaller than the size of the laser beam. *Journal of the American Society for Mass Spectrometry*. 2005; 16:1654–1659. [PubMed: 16095912]
- Kaleta BK, van der Wiel IM, Stauber J, Dekker LJ, Guzel C, Kros JM, Luidert TM, Heeren RM. Sample preparation issues for tissue imaging by imaging MS. *Proteomics*. 2009 Epub.
- Khatib-Shahidi S, Andersson M, Herman JL, Gillespie TA, Caprioli RM. Direct molecular analysis of whole-body animal tissue sections by imaging MALDI mass spectrometry. *Analytical Chemistry*. 2006; 78:6448–6456. [PubMed: 16970320]
- Leinweber BD, Tsapralis G, Monks TJ, Lau SS. Improved MALDI-TOF imaging yields increased protein signals at high molecular mass. *Journal of the American Society for Mass Spectrometry*. 2009; 20:89–95. [PubMed: 18926723]



- Lemaire R, Desmons A, Tabet JC, Day R, Salzet M, Fournier I. Direct analysis and MALDI imaging of formalin-fixed, paraffin-embedded tissue sections. *Journal of Proteome Research*. 2007; 6:1295–1305. [PubMed: 17291023]
- Liu Q, Xiao Y, Pagan-Miranda C, Chiu YM, He L. Metabolite imaging using matrix-enhanced surface-assisted laser desorption/ionization mass spectrometry (ME-SALDI-MS). *Journal of the American Society for Mass Spectrometry*. 2009; 20:80–88. [PubMed: 18926722]
- Minerva L, Clerens S, Baggerman G, Arckens L. Direct profiling and identification of peptide expression differences in the pancreas of control and ob/ob mice by imaging mass spectrometry. *Proteomics*. 2008; 8:3763–3774. [PubMed: 18712771]
- Monroe EB, Annangudi SP, Hatcher NG, Gutstein HB, Rubakhin SS, Sweedler JV. SIMS and MALDI MS imaging of the spinal cord. *Proteomics*. 2008; 8:3746–3754. [PubMed: 18712768]
- Reyzer ML, Hsieh Y, Ng K, Korfmacher WA, Caprioli RM. Direct analysis of drug candidates in tissue by matrix-assisted laser desorption/ionization mass spectrometry. *Journal of Mass Spectrometry*. 2003; 38:1081–1092. [PubMed: 14595858]
- Rubakhin SS, Greenough WT, Sweedler JV. Spatial profiling with MALDI MS: distribution of neuropeptides within single neurons. *Analytical Chemistry*. 2003; 75:5374–5380. [PubMed: 14710814]
- Rubakhin SS, Hatcher NG, Monroe EB, Heien ML, Sweedler JV. Mass spectrometric imaging of the nervous system. *Current Pharmaceutical Design*. 2007; 13:3325–3334. [PubMed: 18045186]
- Rujoi M, Estrada R, Yappert MC. In situ MALDI-TOF MS regional analysis of neutral phospholipids in lens tissue. *Analytical Chemistry*. 2004; 76:1657–1663. [PubMed: 15018564]
- Signor L, Varesio E, Staack RF, Starke V, Richter WF, Hopfgartner G. Analysis of erlotinib and its metabolites in rat tissue sections by MALDI quadrupole time-of-flight mass spectrometry. *Journal of Mass Spectrometry*. 2007; 42:900–909.
- Sjövall P, Lausmaa J, Johansson B. Mass spectrometric imaging of lipids in brain tissue. *Analytical Chemistry*. 2004; 76:4271–4278. [PubMed: 15283560]
- Stauber J, Lemaire R, Franck J, Bonnel D, Croix D, Day R, Wisztorski M, Fournier I, Salzet M. MALDI imaging of formalin-fixed paraffin-embedded tissues: Application to model animals of Parkinson disease for biomarker hunting. *Journal of Proteome Research*. 2008; 7:969–978. [PubMed: 18247558]
- Stoeckli M, Chaurand P, Hallahan DE, Caprioli RM. Imaging mass spectrometry: A new technology for the analysis of protein expression in mammalian tissues. *Nature Medicine*. 2001; 7:493–496.
- Stoeckli M, Staab D, Schweitzer A, Gardiner J, Seebach D. Imaging of a beta-peptide distribution in whole-body mice sections by MALDI mass spectrometry. *Journal of the American Society for Mass Spectrometry*. 2007; 18:1921–1924. [PubMed: 17827032]
- Taban IM, Altelaar AF, van der Burgt YE, McDonnell LA, Heeren RM, Fuchser J, Baykut G. Imaging of peptides in the rat brain using MALDI-FTICR mass spectrometry. *Journal of the American Society for Mass Spectrometry*. 2007; 18:145–151. [PubMed: 17055739]
- Trim PJ, Henson CM, Avery JL, McEwen A, Snel MF, Claude E, Marshall PS, West A, Princivalle AP, Clench MR. Matrix-assisted laser desorption/ionization-ion mobility separation-mass spectrometry imaging of vinblastine in whole body tissue sections. *Analytical Chemistry*. 2009; 80:8628–8634. [PubMed: 18847214]
- Troendle FJ, Reddick CD, Yost RA. Detection of pharmaceutical compounds in tissue by matrix-assisted laser desorption/ionization and laser desorption/chemical ionization tandem mass spectrometry with a quadrupole ion trap. *Journal of the American Society for Mass Spectrometry*. 1999; 10:1315–1321.
- Woods AS, Jackson SN. Brain tissue lipidomics: direct probing using matrix-assisted laser desorption/ionization mass spectrometry. *AAPS Journal*. 2006; 8:E391–395. [PubMed: 16796390]
- Yanagisawa K, Shyr Y, Xu BJ, Massion PP, Larsen PH, White BC, Roberts JR, Edgerton M, Gonzalez A, Nadaf S, Moore JH, Caprioli RM, Carbone DP. Proteomic patterns of tumour subsets in non-small-cell lung cancer. *The Lancet*. 2003; 362:415–416.
- Zimmerman TA, Monroe EB, Sweedler JV. Adapting the stretched sample method from tissue profiling to imaging. *Proteomics*. 2008; 8:3809–3815. [PubMed: 18712762]

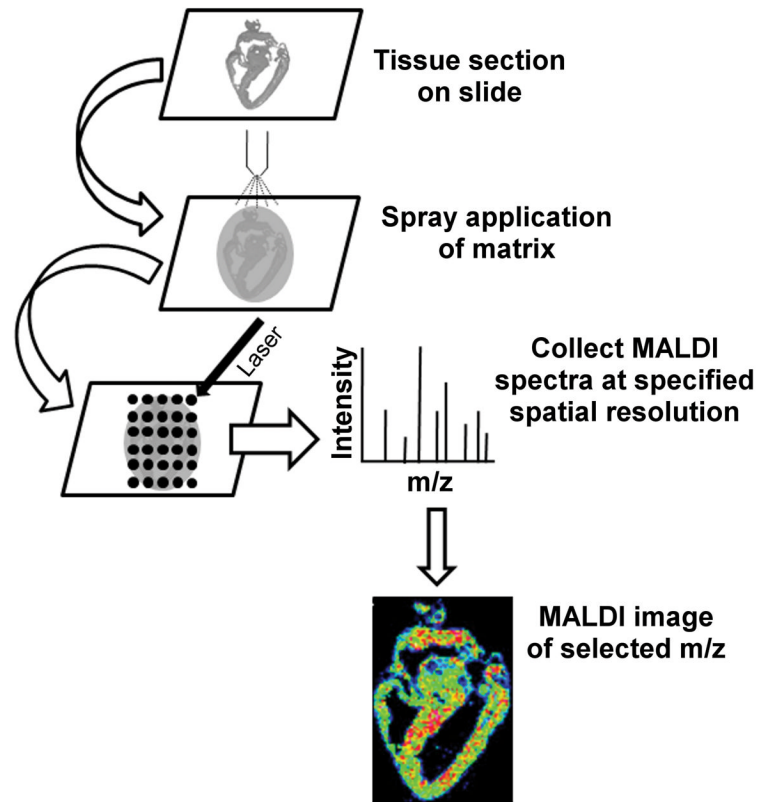


**Figure 1. Workflow for MALDI Imaging Experiment**

Tissue sections are mounted on MALDI target and matrix is applied by spray coating. MALDI mass spectra are acquired at a specified spatial resolution (75–100  $\mu\text{m}$  in the present study). Plots of spectral intensity and location for a specified m/z value produce a MALDI image.

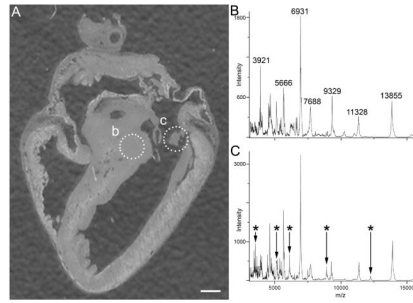


**Figure 2. Extracted MALDI Mass Spectra with CHCA matrix**

(A) Optical image of chick heart showing regions of interest (dotted circles) from which mass spectra were extracted. (B) MALDI mass spectrum of the bundle of His region. (C) MALDI mass spectrum of a heart valve structure. Major differences in the mass spectra are indicated by asterisks. Scale bar = 1 mm.

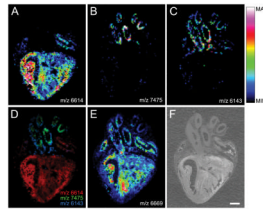


**Figure 3. Chick Heart Imaging Mass Spectrometry with DHB matrix**

(A) The protein signal at  $m/z$  6614 is expressed predominantly in the myocardium. In contrast, the protein signals at  $m/z$  7475 and  $m/z$  6143 are expressed predominantly in the major heart vessels (B and C, respectively). Interestingly,  $m/z$  7475 and  $m/z$  6143 are expressed in different regions of the vasculature. (D) An overlay image of protein signals at  $m/z$  6614 (red),  $m/z$  7475 (green) and  $m/z$  6143 (blue) showing their spatial relationship to each other. (E) In contrast, the protein signal at  $m/z$  6669 is found throughout the chick heart. (F) Optical image of the chick heart tissue section prior to application of matrix solution. Intensity scale applies to panels A–C and E. Scale bar = 1 mm.

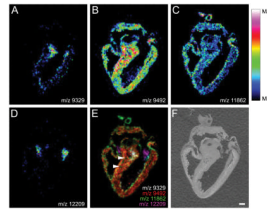


**Figure 4. Chick Heart Imaging Mass Spectrometry with CHCA matrix**

(A) The protein signal at  $m/z$  9329 is localized to the bundle of His. (B) The protein signal at  $m/z$  9492 shows an even distribution throughout the myocardium. (C) The protein signal at  $m/z$  11862, while expressed in the myocardium, is also localized to the walls of the major vessels of the heart. (D) A signal at  $m/z$  12209 was localized to valve structures. (E) An overlay image of protein signals at  $m/z$  9329 (white),  $m/z$  9492 (red),  $m/z$  11862 (green), and  $m/z$  12209 (magenta) showing their spatial relationship to each other. The signal at  $m/z$  11862 is also localized to coronary arteries (arrowheads). (F) The chick heart tissue section prior to application of matrix solution. Intensity scale applies to panels A–D. Scale bar = 1 mm.



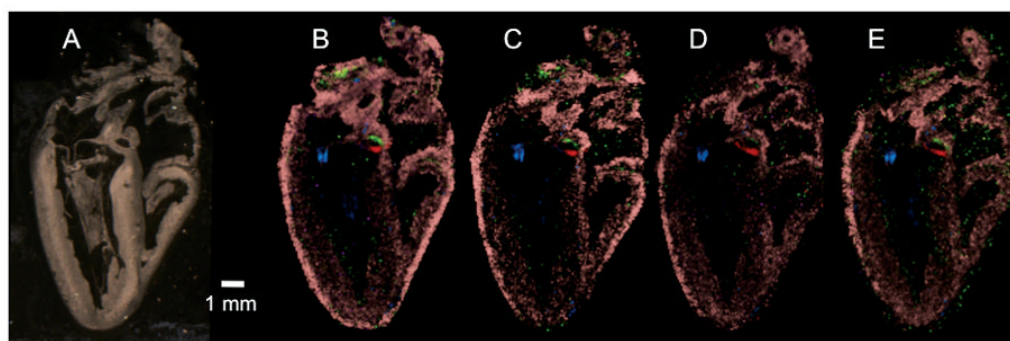


**Figure 5. Reproducibility study using SA matrix**

(A) Optical image of chick heart section subsequently sprayed with matrix and imaged. (B–E) Four MALDI images from serial sections of a chick heart coated with SA matrix. Four protein signals are plotted in each image to demonstrate spatial resolution and reproducibility of the method:  $m/z$  3915 (blue),  $m/z$  5935 (red),  $m/z$  5308 (green), and  $m/z$  6643 (pink). Scale bar = 1 mm.